Resonant Majorana neutrino effects in $\Delta L = 2$ four-body hyperon decays

Gerardo Hernández-Tomé,[1] Diego Portillo-Sánchez,[2] and Genaro Toledo[1]

[1]*Instituto de Física, Universidad Nacional Autónoma de México, AP 20-364, Ciudad de México 01000, México*

[2]*Departamento de Física, Centro de Investigación y de Estudios Avanzados del Instituto Politécnico Nacional, Apartado Postal 14-740, 07000 México D.F., México*

(Received 15 December 2022; accepted 14 March 2023; published 29 March 2023)

We computed the $\Sigma^- \to n\pi^+ e^- \ell^-$ ($\ell = e,\ \mu$), $\Xi^- \to \Lambda\pi^+ e^- e^-$, and $\Lambda \to p\pi^+ e^- e^-$ lepton number violating (LNV) hyperon decays mediated by a resonant Majorana neutrino. The expected hyperon production rate of experiments like BESIII of around 10^6–10^8 may allow searching for these rare hyperon decays at enough sensitivities. We illustrate the limits on the new heavy mixing parameters derived from these hyperon channels and compare them with other LNV meson decays in similar mass regions of the resonant neutrino state.

DOI: 10.1103/PhysRevD.107.055042

I. INTRODUCTION

The study of hyperon decay properties had a golden era some sixty years ago when Cabibbo proposed the universality of charged weak interactions in semileptonic decays [1]. Hyperon semileptonic decays were used to measure the weak charges in strangeness-changing transitions and to extract the Cabibbo angle $\sin\theta_c$. On the other hand, nonleptonic decays were considered to measure the hyperon polarizations and to determine the final state interaction phases [2–4]. The field of hyperon physics was somehow abandoned with the advent of high intensity kaon beams, which allowed to extract the Cabibbo angle with reduced strong interaction uncertainties. Until the late nineties, only a few searches of rare and forbidden hyperon decays were reported [5]. In the last twenty-five years, a few more data on allowed, rare, and forbidden hyperon decays were reported by the HyperCP [6], NA48 [7], LHCb [8], KTeV [9], and BESIII [10,11] Collaborations.

The BESIII hyperon physics program has brought a renewed interest in this field thanks to the large dataset of baryon-antibaryon pairs produced in J/ψ and $\psi(2S)$ decays [10]. Owing to the non-negligible branching fractions for these decays, the large production rate of these charmonium states would allow the production of 10^6–10^8 hyperon pairs of different species. This opens the possibility of improving measurements of allowed and rare hyperon decays that will set strong limits, for example, on the rare flavour changing neutral currents hyperon decays with charged lepton or neutrinos pairs [10]. Similarly, searches for forbidden (lepton number or baryon number) decays can be pursued, allowing to test models that include the violation of these accidental symmetries [10].

At present, the observation of neutrino oscillation represents one of the most thrilling discoveries in particle physics, setting new questions about the nature and origin of their tiny masses. The most promising approach to establish if neutrinos are their own antiparticles is to search for lepton number violating processes ($\Delta L = 2$), which would be only possible if that is the case. Despite the neutrinoless double Beta decays in nuclei, ($0\nu\beta\beta$) are the most extensively studied and promising laboratory to give an answer on this matter; alternative and complementary searches for other lepton number violating (LNV) processes can also play a crucial role in current and future experiments since they provide information on specific energy windows.

In this paper we focus on the $B_A(p_A) \to B_B(p_B) \times \ell_1^-(p_1)\ell_2^-(p_2)\pi^+(p_\pi)$ LNV decays ($B_{A,B}$ denote hyperon states, see Fig. 1). Specifically, we will consider the following channels: $\Sigma^- \to n\pi^+ e^- \ell^-$ ($\ell = e,\ \mu$), $\Xi^- \to \Lambda\pi^+ e^- e^-$, and $\Lambda \to p\pi^+ e^- e^-$. These kinds of decays have not been studied before, and they can be induced by the resonant enhancement of intermediate mass Majorana neutrinos.[1] LNV hyperon decays of the form $B_A^- \to B_B^+ \ell^- \ell'^-$ have been studied before in Refs. [31–34]. These processes are mediated by a virtual Majorana neutrino and are similar to neutrinoless double Beta decays.

[1]These novel channels extend the search of similar LNV effects performed in semileptonic baryon, meson, and tau decays [12–30].

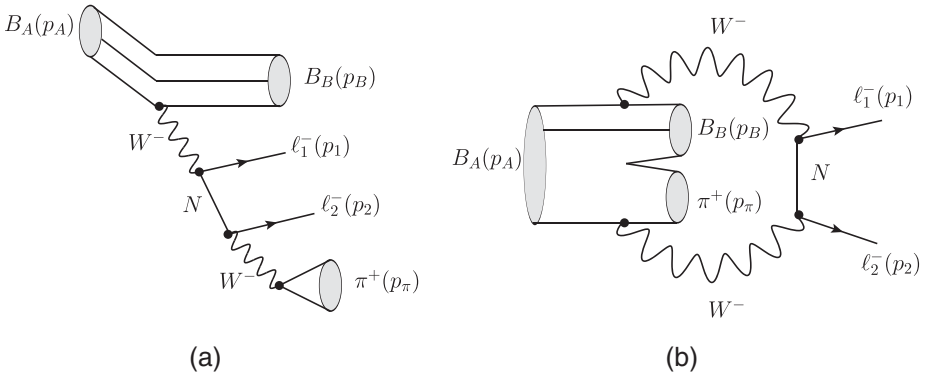

FIG. 1. Feynman diagrams for the four-body $\Delta L = 2$ hyperon decays mediated by a resonant heavy Majorana neutrino N. We consider the following channels: $\Sigma^- \to n\pi^+ e^- \ell^-$ ($\ell = e, \mu$), $\Xi^- \to \Lambda\pi^+ e^- e^-$, and $\Lambda \to p\pi^+ e^- e^-$. Note that diagram (a) is the dominant one when the neutrino is on shell because its contribution is enhanced due to a resonance effect, opposite to diagram (b) where the neutrino cannot become a resonant state.

On the other hand, resonant production of Majorana neutrinos are possible for a limited range of their masses in such a way that they can be produced on their mass shell. Contrary to production of virtual Majorana neutrino processes with rates of $O(G_F^4)$, the rates for production of resonant Majorana neutrinos becomes of $O(G_F^2)$ [12,18], which allows to place better constraints of their parameter space even with upper limits given by current experimental sensitivities.

In the following we present the formalism to describe these processes and introduce the integration method for four-body decays, which extend the one followed in the three-body case [12,18] and allows to properly account for the different charged lepton's flavor case. Given the clean experimental signature, one may expect that very strong limits can be set on the branching fractions of these decays, similar to existing limits on other $\Delta L = 2$ meson decays. Therefore, it would be interesting to explore if similar limits on the parameter space of resonant Majorana neutrinos can be obtained from the proposed four-body hyperon decays.

II. COMPUTATION

Adopting the convention for the neutrino states on Ref. [12], let us consider a scenario where the leptonic sector incorporates a number n of singlet right-handed neutrinos, N_{R_j} ($j = 1, 2, \ldots n$), in addition to the usual three left-handed $SU(2)$ lepton doublets $L_{iL}^T = (\nu_i, \ell_i)_L$. In such scenario, after the proper mass matrix diagonalization, the charged lepton current relevant for our computation can be written as follows:

$$\mathcal{L}_W = -\frac{g}{\sqrt{2}} W^+ \left(\sum_{\ell=e,\mu,\tau} \sum_{i=1}^{3} U_{\ell i}^* \overline{\nu_i} \gamma_\mu P_L \ell + \sum_{\ell=e,\mu,\tau} \sum_{j=4}^{3+n} V_{\ell j}^* \overline{N_j^c} \gamma_\mu P_L \ell \right) + \text{H.c.}, \quad (2.1)$$

where $P_L = (1-\gamma_5)/2$ is the left-handed chirality projector, $N^c = C\bar{N}^T$ is the charge conjugate spinor, and $U_{\ell j}$ ($V_{\ell j}$) describes the lepton mixing matrix elements for the light (heavy) neutrino states.

Similar to previous works, we base our analysis on considering the case of a simply minimal scenario with only one heavy Majorana neutrino N, with the corresponding mass m_N and mixing with the charged lepton flavor $V_{\ell N}$ ($\ell = e, \mu, \tau$).[2] The relevant diagram for the $B_A(p_A) \to B_B(p_B)\ell_1^-(p_1)\ell_2^-(p_2)\pi^+(p_\pi)$ LNV hyperon decays is depicted in Fig. 1(a), and its amplitude can be written as follows:

$$\mathcal{M}_1 = \left(\frac{G V_{\ell_1 N} V_{\ell_2 N} f_\pi m_N}{a_1 + i\Gamma_N m_N} \right) \ell_{\mu\nu}(p_1, p_2) H^\mu(p_B, p_A) p_\pi^\nu, \quad (2.2)$$

where $a_1 \equiv (p_A - p_B - p_1)^2 - m_N^2$, and $p_A - p_B - p_1 = p_\pi + p_2$ is the momentum carried out by the heavy neutrino N, and we have defined $G \equiv G_F^2 V_{us} V_{ud}$. The leptonic and hadronic parts are given by

$$\ell_{\mu\nu}(p_1, p_2) \equiv \bar{u}(p_1)\gamma_\mu\gamma_\nu(1+\gamma_5)v(p_2), \quad (2.3)$$

$$H^\mu(p_B, p_A) \equiv \langle B_B(p_B)|J_\mu|B_A(p_A)\rangle. \quad (2.4)$$

The hadronic current J_μ is parametrized in terms of six form factors which are determined from the well-known lepton number conserving hyperon decays $B_A \to B_B \ell^- \bar{\nu}_\ell$ ($\ell = e, \mu$) [39–42]:

[2]This minimal scenario is not able to explain the current data coming from neutrino oscillation experiments but represents a simple approach to encode the effects of a larger number of heavy states present in well-justified massive neutrino models. Recently, the interference effects in extensions with at least two heavy neutrino states for three-body meson LNV decays have been reported in [35–38].

$$\langle B_B(p_B)|J_\mu|B_A(p_A)\rangle = \bar{u}(p_B)\left[f_1(q^2)\gamma_\mu + if_2(q^2)\frac{\sigma_{\mu\nu}q^\nu}{M_A} + \frac{q_\mu f_3(q^2)}{M_A} + g_1(q^2)\gamma_\mu\gamma_5 + ig_2(q^2)\frac{\sigma_{\mu\nu}q^\nu\gamma_5}{M_A} + \frac{q_\mu g_3(q^2)\gamma_5}{M_A}\right]u(p_A), \tag{2.5}$$

where $q^2 = (p_A - p_B)^2$ is the squared momentum transferred in the hadronic transition, $u(p_A)$ and M_A ($\bar{u}(p_B)$, and M_B) are the spinor and mass of the initial (final) baryon, respectively. Nevertheless, the contributions of f_3 and g_3 form factors in Eq. (2.5) are negligible in comparison with the other form factors since they pick up a factor proportional to the mass of the charged-lepton m_ℓ involved in the transition [39–41]. Furthermore, f_2 and g_2 are, in principle, not negligible, but they become subleading in the SU(3)-flavor symmetry of QCD [43,44]. Therefore, in the following we will consider that the hadronic current describing the hadronic transition in Eq. (2.4) is dominated by the vector and axial form factors as follows:

$$\langle B_B(p_B)|J_\mu|B_A(p_A)\rangle = \bar{u}(p_B)\gamma_\mu[f_1(q^2) + g_1(q^2)\gamma_5]u(p_A). \tag{2.6}$$

Now, from neutrino and electron scattering off nucleons it has been found that the observed distributions can be described by a dipole parametrization. In such a way that an extrapolation to the timelike region leads to

$$f_1(q^2) = f_1(0)\left(1 - \frac{q^2}{m_{df}^2}\right)^{-2}, \tag{2.7}$$

$$g_1(q^2) = g_1(0)\left(1 - \frac{q^2}{m_{dg}^2}\right)^{-2}, \tag{2.8}$$

with $m_{df} = 0.84$ GeV and $m_{dg} = 1.08$ GeV. Since these pole masses correspond to strangeness-conserving form factors, a rescaling using the values of vector and axial meson masses allows to assume that $m_{df} = 0.97$ GeV and $m_{dg} = 1.25$ GeV would be a good guess for the dipole masses in the strangeness-changing case [39,40]. The values of the form factors at zero momentum transfer, $f_1(0)$ and $g_1(0)$, are given in Table I, and in the case of the vector form factors they incorporate the effects of SU(3) flavor symmetry breaking [39–42].

It is important to note that the amplitude $\mathcal{M}_1$ in Eq. (2.2) has a resonant effect when $(p_\pi + p_2)^2 \approx m_N^2$.[3] Besides, if the experiment is unable to distinguish which lepton was emitted at each stage for nonidentical charged leptons or for the antisymmetrization of identical leptons, then we also need to consider the diagram contribution with the final charged leptons interchanged $\ell_1(p_1) \leftrightarrow \ell_2(p_2)$ in Fig. 1. This second diagram has a resonant effect when $(p_\pi + p_1)^2 \approx m_N^2$. Since, in general, $(p_\pi + p_2)^2 \neq (p_\pi + p_1)^2$, it turns out convenient to apply the single-diagram-enhanced multichannel integration method [45]. This method has been implemented for three-body channels. Here we generalize it to four-body decays, along the same lines by defining the functions

TABLE I. Vector and axial transition form factors for weak hyperon decays at zero momentum transfer ($q^2 = 0$) [39].

Transition	$f_1(0)$	$g_1(0)$
$\Sigma^- \to n$	-1	0.341
$\Xi^- \to \Lambda$	$\sqrt{3/2}$	0.239
$\Lambda \to p$	$-\sqrt{3/2}$	−0.895

$$f_{PS_1} = \frac{\overline{|\mathcal{M}_1|}^2}{\overline{|\mathcal{M}_1|}^2 + \overline{|\mathcal{M}_2|}^2}\overline{|\mathcal{M}|}^2,$$
$$f_{PS_2} = \frac{\overline{|\mathcal{M}_2|}^2}{\overline{|\mathcal{M}_1|}^2 + \overline{|\mathcal{M}_2|}^2}\overline{|\mathcal{M}|}^2, \tag{2.9}$$

with $\mathcal{M} = \mathcal{M}_1 + \mathcal{M}_2$. In this way, Eq. (A3) can be rewritten as $\overline{|\mathcal{M}|}^2 = f_{PS_1} + f_{PS_2}$, and consequently, the decay width is given by

$$\Gamma_{B_A\to B_B\ell_1^-\ell_2^-\pi^+} = \frac{N}{4(4\pi)^6 m_A^3}\left[\int f_{PS_1} dPS_1 + \int f_{PS_2} dPS_2\right], \tag{2.10}$$

with $N = 1/2, (1)$ for the case where the two charged final leptons are the same (different) particles. In our case, the functions f_{PS_1} and f_{PS_2} can be written as follows (see Appendix A for details):

$$f_{PS_1} = \frac{(GV_{\ell_1 N}V_{\ell_2 N}f_\pi m_N)^2 A}{a_1^2 + \Gamma_N^2 m_N^2} \times \left[1 + 2\frac{(a_1a_2 + \Gamma_N^2 m_N^2)C_1 + (a_2 - a_1)\Gamma_N m_N C_2}{(a_2^2 + \Gamma_N^2 m_N^2)A + (a_1^2 + \Gamma_N^2 m_N^2)B}\right], \tag{2.11}$$

$$f_{PS_2} = f_{PS_1}(p_1 \leftrightarrow p_2), \tag{2.12}$$

where the A, B, C_1, and C_2 functions are reported for the first time in Appendix A. Now, the phase space integration

[3]For the $B_A(p_A) \to B_B(p_B)\ell_1^-(p_1)\ell_2^-(p_2)\pi^+(p_\pi)$ decays mediated by an intermediate neutrino state produced on shell, its mass must satisfy that $m_{\ell_2^-} + m_{\pi^+} \leq m_N \leq m_A - m_B - m_{\ell_1^-}$.

can be done for f_{PS_1} and f_{PS_2} separately and added up after the proper phase space integration. Regarding the first integral in Eq. (2.10),[4] this is described conveniently in terms of the five independent variables $(s_{B1}, s_{2\pi}, \theta_B, \theta_2, \phi)$ (see Fig. 1 in Ref. [46]):

(i) $s_{B1} = (p_B + p_1)^2$ and $s_{2\pi} = (p_2 + p_\pi)^2$ stand for the invariant masses of the $B_B\ell_1^-$ and $\ell_2^-\pi^+$ systems, respectively.

(ii) θ_B (θ_2) is the angle between the three-momenta of B_B (π^+) in the rest frame of the pair $B_B\ell_1^-$ ($\pi^+\ell_2^-$) with respect to the line of flight of the $B_B\ell_1^-$ ($\pi^+\ell_2^-$) in the rest frame of the particle B_A.

(iii) ϕ is the angle between the planes defined by the $B_B\ell_1^-$ and $\pi^+\ell_2^-$ pair systems in the rest frame of the particle B_A.

In order to evaluate Eq. (2.10) we need to consider the total decay width for the new heavy neutrino states. This can be obtained by adding up the contributions of all its partial decay widths ($\Gamma_i^{\text{p.w.}}$) that can be opened at the mass m_N [12],

$$\Gamma_N = \sum_i \Gamma_i^{\text{p.w.}} \cdot \theta\left(m_N - \sum_j m_j\right), \tag{2.13}$$

where θ is the Heaviside function, and m_j stand for the masses of all the final states particles involved in $\Gamma_i^{\text{p.w.}}$. Let us illustrate this point by considering the $\Sigma^- \to n\pi^+e^-e^-$ channel; here, the mass of the resonant state must be inside the range $m_{e^-} + m_{\pi^+} \le m_N \le m_{\Sigma^-} - m_n - m_{e^-}$, then the possible decay channels of the heavy N state (induced by charged and neutral currents) that contribute to its total decay width Γ_N are the following: $N \to \ell^\pm\pi^\mp$, $N \to \pi^0\nu_\ell$, $N \to \ell_1^\mp\ell_2^\pm\nu_{\ell_2}$, $N \to \ell_2^-\ell_2^+\nu_{\ell_1}$, and $\nu_{\ell_1}\nu\bar{\nu}$ (with $\ell, \ell_1, \ell_2 = e, \mu$.). The analytical expressions for these partial widths can be found in Ref. [12]; they depend on each particular channel considered, and they are given as a function of both the neutrino mass and the norm of the squared mixings involved, that is, $\Gamma_i^{\text{p.w}} = \Gamma_i^{\text{p.w}}(m_N, |V_{\ell N}|^2)$. Then we have considered the indirect limits on the mixing elements of the heavy neutrino with the three charged leptons [47] in order to estimate the total neutrino width, namely,

$$|V_{eN}| \le 0.050, \quad |V_{\mu N}| \le 0.021, \quad |V_{\tau N}| \le 0.075. \tag{2.14}$$

Using the above values in Eq. (2.13), the total decay width Γ_N varies from 0.07 neV to 4.4 neV into the resonant mass region for the $\Sigma^- \to n\pi^+e^-e^-$ decay. The decay width is very small compared with the mass of the new neutral state $\Gamma_N \ll m_N$, and since $(p_2 + p_\pi)^2 = s_{2\pi} \approx m_N^2$ in Eq. (2.11), the narrow width approximation can be applied. That means that we can replace

$$\frac{1}{(s_{2\pi} - m_N^2)^2 + m_N^2\Gamma_N^2} \to \frac{\pi}{m_N\Gamma_N}\delta(s_{2\pi} - m_N^2), \tag{2.15}$$

transforming the five-variable integral in Eq. (2.11) into a four-variable one:

$$\begin{aligned}\int f_{PS_1} dPS_1 = {} & \frac{\pi(GV_{\ell_1 N}V_{\ell_2 N}f_\pi m_N)^2}{\Gamma_N m_N}\int X\beta_{B1}\beta_{2\pi} \\ & \times \left[A\left(1 + 2\frac{\Gamma_N^2 m_N^2 C_1 + \Gamma_N m_N a_2 C_2}{(a_2^2 + \Gamma_N^2 m_N^2)A + \Gamma_N^2 m_N^2 B}\right)\right] \\ & \times ds_{B1}\, d\cos\theta_B\, d\cos\theta_2\, d\phi,\end{aligned} \tag{2.16}$$

with the following integration limits:

$$\begin{aligned}(m_B + m_1)^2 \le s_{B1} \le (m_A - m_2 - m_\pi)^2, \quad & -1 \le \cos\theta_B \le 1, \\ -1 \le \cos\theta_2 \le 1, \quad & -\pi \le \phi \le \pi.\end{aligned} \tag{2.17}$$

This provides all the formalism we need to compute the decay width and set the region of the parameters, given on the expected experimental branching ratio, as we show below.

III. NUMERICAL ANALYSIS

The projected sensitivity of BESIII for the search of rare and forbidden hyperon three-body hyperon decays at BESIII is of the order of 10^{-6}–10^{-8} [10] with clean backgrounds.[5] However, there is not an estimation for similar four-body hyperon decays. In this work, we will assume an optimistic scenario considering similar sensitivities for three- and four-body processes.

In Fig. 2 we show the exclusion region on the plane (m_N, $|V_{eN}|^2$) for the neutrino resonant state obtained by assuming a rate of $\text{BR}(B_A \to B_B\pi^+e^-e^-) < 10^{-8}$ for the channels involving a pair of electrons in the final state. We have considered here two benchmarks to evaluate the total neutrino width. On one side, the solid lines represent the universal coupling assumption, that is, we consider that $V_{eN} = V_{\mu N} = V_{\tau N}$ in Eq. (2.13); therefore, the total neutrino width (and, consequently, the branching ratio of the $B_A \to B_B\pi^+e^-e^-$ hyperon decays) can be expressed only as a function of $\Gamma_N = \Gamma_N(|V_{eN}|^2, m_N)$. On the other hand, the dashed lines represent a scenario where the total neutrino width is fixed to the reasonable value

[4]The phase space variables for the second integral in Eq. (2.10) are chosen conveniently as $(s_{B2}, s_{1\pi}, \theta_B, \theta_1, \phi)$ with the mass invariants $s_{B2} = (p_B + p_2)^2$, and $s_{1\pi} = (p_1 + p_\pi)^2$.

[5]It is also worthy to mention that these kinds of transitions can also be searched by the LHCb Collaboration with higher sensitivities because of the huge production cross section there.

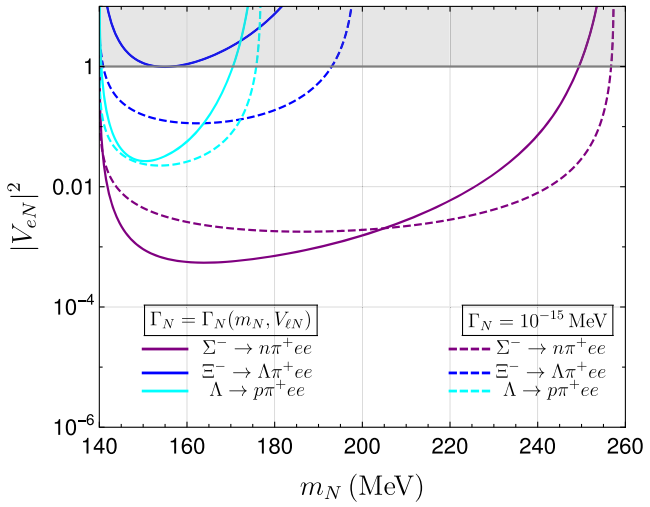

FIG. 2. Exclusion regions on the $(m_N, |V_{eN}|^2)$ plane by assuming a $\mathrm{BR}(B_A \to B_B\pi^+e^-e^-) < 10^{-8}$ limit. The purple line stands for the $\Sigma^- \to \pi^+ne^-e^-$ channel, the blue one for the $\Xi^- \to \Lambda\pi^+e^-e^-$, and the cyan color for the $\mathrm{BR}(\Lambda \to p\pi^+e^-e^-)$ decay (see main text for further details). The solid (dashed) lines correspond to estimates considering a parameter's dependent neutrino width Γ_N (fixed). Notice that values where $|V_{eN}| > 1$ do not have a physical meaning. The shadow area just illustrates that a sensibility of 10^{-8} for the branching ratio of the $\Xi^- \to \Lambda\pi^+ee$ channel is insufficient to set bounds in that scenario.

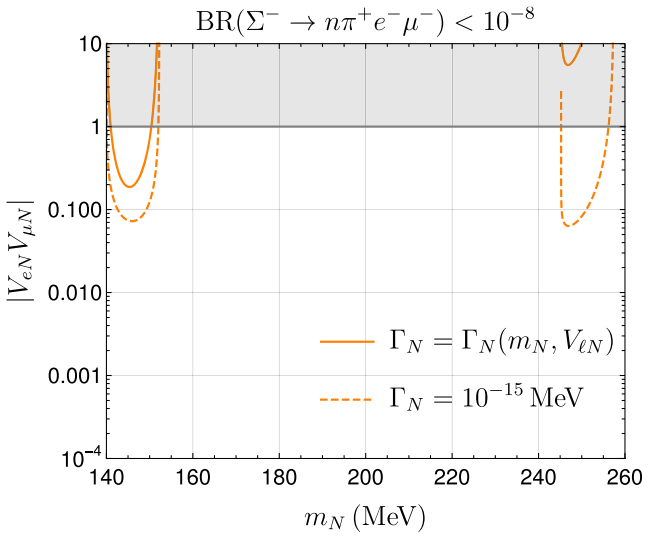

FIG. 3. Same as Fig. 2 but for the exclusion regions on the $(m_N, |V_{eN}V_{\mu N}|)$ plane by assuming the $\mathrm{BR}(\Sigma^- \to n\pi^+e^-\mu^-) < 10^{-8}$ limit in the search of lepton flavor violating hyperon decays.

$\Gamma_N = 10^{-15}$ MeV [consistent with the estimation of the total neutrino width using the indirect limits reported in Eq. (2.14)]. From this plot, we can observe that, in general, the exclusion region will depend on which assumption we considered, although in general, they are of the same order for all the allowed mass of the resonant neutrino in the different channels. In any case, the most restrictive limits will come from the $\Sigma^- \to n\pi^+e^-e^-$ channel, followed by $\Lambda \to p\pi^+e^-e^-$, and finally the much less restrictive $\Xi^- \to \Lambda\pi^+e^-e^-$ channel. Additionally, to the processes with a pair of electrons in the final state, the $\Sigma^- \to n\pi^+e\mu^-$ channel is the only possible kinematically allowed four-body LNV hyperon decay. As we can see in Fig. 3, if the search for this transition can achieve a rate of $\mathrm{BR}(\Sigma^- \to n\pi^+e^-\mu^-) < 10^{-8}$, then the limits set on the plane $(m_N, |V_{eN}V_{\mu N}|)$ are much less restrictive than the dielectronic case because phase space restrictions are more stringent. For the case with two different flavors, notice that the limits are split into two disconnected regions. The left (right) region on Fig. 3, is associated with the case where the muon (electron) was created along with the resonant neutrino state, and the electron (muon) comes after the subsequent neutrino decay. Overlap of these regions can be achieved in other scenarios, provided the kinematical conditions allow them to do so. The formalism developed here allows to address both cases regardless of invoking the direct narrow width approximation or not (see Appendix B).

It is important to mention that despite the assumed sensitivity (10^{-8}) for the branching ratio of the four-body $B_A(p_A) \to B_B(p_B)\ell_1^-(p_1)\ell_2^-(p_2)\pi^+(p_\pi)$, hyperon channels studied here are around 3 orders smaller than three-body LNV kaon decays $K^+ \to \pi^-\ell_1^+\ell_2^+$[6]; the upper bounds on the $|V_{\ell N}|^2$ mixings excluded by the present calculation in the range of mass showed in Figs. 2 and 3 are significantly less restrictive. This is owing to the phase space suppression of the intermediate $B_A \to B_B\ell_1 N$ hyperon process in comparison with the $K^+ \to \ell_1 N$ channel.

On the other hand, our results exhibit that upper bounds on the $|V_{\ell N}|^2$ mixings from these kinds of decays are comparable with the ones obtained from three-body $\Delta L = 2$ decays of (D^+, D_s^+, B^+) mesons. Note that the current advantage of the kaon system, triggered by its particular features both theoretically and experimentally, results from pioneering work that led to theoretical and experimental control of their features.

To our knowledge, the hyperon decays are starting to be explored for this kind of physics, then four-body hyperon decays with $\Delta L = 2$ can be searched in BESIII as a clear experimental signal with charged particles and eventually be used to constrain other models with lepton number violations. On this matter, we envisage growing theoretical and experimental efforts that may also lead to a competitive scenario.

IV. CONCLUSIONS

The search for $\Delta L = 2$ processes is crucial for unraveling the Dirac or Majorana nature of neutrinos. Except

[6]Current bounds for $K^+ \to \pi^-e^+e^+ \leq 5.3 \times 10^{-11}$ and $K^+ \to \pi^-e^+\mu^+ \leq 4.2 \times 10^{-11}$ are reported by the NA62 experiment at CERN in [48,49].

possibly for neutrinoless double-beta decay in nuclei, diverse neutrino mass models predict that LNV effects can lie beyond the reach of current experiments. However, if new hypothetical heavy Majorana neutrinos with masses from ∼100 MeV to few GeV can be produced on shell as an intermediate state in LNV decays of mesons, baryons, or the tau lepton, then their branching ratios can be amplified due to a resonant effect. The no observation of such processes sets limits on the parameter space of these new heavy neutrinos states. In this regard, most of the studies have focused on three-body LNV meson or tau decays, however, recently the study of similar four-body LNV channels has also drawn attention as complementary means because they can provide information about different kinematical phase space regions. In this work, we studied the four-body LNV decays of hyperons mediated by a resonant Majorana neutrino.

Our results suggest that the direct limits derived on $|V_{eN}|^2$ from the $\Sigma^- \to n\pi^+e^-e^-$ channel can be of the same order ($\sim 10^{-3}$) as those obtained from the meson decays, such as $D^+ \to \pi^-e^+e^+$ and $D_s^+ \to \pi^-e^+e^+$, but far from the current most stringent ones from the semileptonic kaon decay $K^+ \to \pi^-e^+e^+$, which is around $\mathcal{O}(10^{-9})$ [18]. Moreover, less restrictive limits on $|V_{eN}|^2$ ($\sim 10^{-1}$) can be obtained from the $\Lambda \to p\pi^+e^-e^-$ and $\Xi^- \to \Lambda\pi^+e^-e^-$, which are comparable with the limits from the $B^+ \to \pi^-e^+e^+$ meson channel. On the other hand, the $\Sigma^- \to n\pi^+e^-\mu^-$ channel is the only possible four-body LNV hyperon decay mediated by a Majorana neutrino involving a muon as the final state, but it places very weak constraints on $|V_{eN}V_{\mu N}|$ for the small mass on-shell neutrino regions allowed, assuming the expected sensitivity for rare hyperon decays of BESIII.

ACKNOWLEDGMENTS

We would like to thank G. López Castro for many helpful discussions. G. H.-T. and G. T. acknowledge the support of DGAPA-PAPIIT UNAM, Grant No. IN110622 for financial support. G. H.-T. is funded by PROGRAMA DE BECAS POSDOCTORALES DGAPA-UNAM. The work of D. P.-S. was supported by Ciencia de Frontera Conacyt Project No. 428218 and the program "BECAS CONACYT NACIONALES."

APPENDIX A: AMPLITUDES OF FOUR-BODY $\Delta L = 2$ HYPERON DECAYS

Following the Feynman rules for fermion number-violating interactions reported in Ref. [50], the contribution of the second diagram with the charged leptons interchanged in Fig. 1(a) is given by

$$\mathcal{M}_2 = \left(\frac{GV_{\ell_1 N}V_{\ell_2 N}f_\pi m_N}{a_2 + i\Gamma_N m_N}\right)\ell_{\nu\mu}(p_1,p_2)H^\mu(p_B,p_A)p_\pi^\nu, \tag{A1}$$

with $a_2 \equiv (p_A - p_B - p_2)^2 - m_N^2$. Therefore, $\mathcal{M} = \mathcal{M}_1 + \mathcal{M}_2$ can be written as follows:

$$\mathcal{M} = GV_{\ell_1 N}V_{\ell_2 N}f_\pi m_N \bar{u}(p_1)\left(\frac{\gamma_\mu\gamma_\nu}{a_1 + i\Gamma_N m_N} + \frac{\gamma_\nu\gamma_\mu}{a_2 + i\Gamma_N m_N}\right)(1+\gamma_5)v(p_2)H^\mu(p_B,p_A)p_\pi^\nu. \tag{A2}$$

The total amplitude squared is given by

$$\overline{|\mathcal{M}|}^2 = \frac{1}{2}\sum_{\text{spins}}|\mathcal{M}|^2 = \frac{1}{2}\sum_{\text{spins}}(|\mathcal{M}_1|^2 + |\mathcal{M}_2|^2 + 2\text{Re}[\mathcal{M}_1\mathcal{M}_2^\dagger]), \tag{A3}$$

where the individual contributions can be written as follows:

$$\begin{aligned}\overline{|\mathcal{M}_1|}^2 &= \frac{1}{2}\sum_{\text{spins}}|\mathcal{M}_1|^2 = \frac{1}{2}\frac{(GV_{\ell_1 N}V_{\ell_2 N}f_\pi m_N)^2 A}{(a_1^2 + \Gamma_N^2 m_N^2)},\\ \overline{|\mathcal{M}_2|}^2 &= \frac{1}{2}\sum_{\text{spins}}|\mathcal{M}_2|^2 = \frac{1}{2}\frac{(GV_{\ell_1 N}V_{\ell_2 N}f_\pi m_N)^2 B}{(a_2^2 + \Gamma_N^2 m_N^2)},\end{aligned} \tag{A4}$$

while the interference term,

$$\mathcal{M}_1\mathcal{M}_2^\dagger = (GV_{\ell_1 N}V_{\ell_2 N}f_\pi m_N)^2(C_1 + iC_2)\frac{[a_1a_2 + \Gamma_N^2 m_N^2 + i(a_1 - a_2)]\Gamma_N m_N}{(a_1^2 + \Gamma_N^2 m_N^2)(a_2^2 + \Gamma_N^2 m_N^2)}, \tag{A5}$$

with the A, B, C_1, and C_2 functions given by

$$A = 64[f_1^2(q^2)\xi_1 + g_1^2(q^2)\xi_2 + f_1(q^2)g_1(q^2)\xi_3], \quad \text{(A6)}$$

$$B = A(p_1 \leftrightarrow p_2), \quad \text{(A7)}$$

$$C_1 = 64[f_1^2(q^2)\xi_4 + g_1^2(q^2)\xi_5 + f_1(q^2)g_1(q^2)\xi_6],$$
$$C_2 = 64\epsilon_{\mu\nu\lambda\rho}p_B^\mu p_1^\nu p_2^\lambda p_\pi^\rho[-(f_1^2 + g_2^2)(r_{A\pi} + r_{B\pi}) + f_1(q^2)g_1(q^2)2(r_{1\pi} + r_{2\pi})], \quad \text{(A8)}$$

and the following definitions:

$$\xi_1 = m_A m_B(m_\pi^2 r_{12} - 2r_{1\pi}r_{2\pi}) - m_\pi^2(r_{A1}r_{B2} + r_{A2}r_{B1}) + 2r_{2\pi}(r_{A1}r_{B\pi} + 2r_{A\pi}r_{B1}), \quad \text{(A9)}$$

$$\xi_2 = \xi_1 - 2m_A m_B(m_\pi^2 r_{12} - 2r_{12}r_{2\pi}), \quad \text{(A10)}$$

$$\xi_3 = 2[m_\pi^2(r_{A2}r_{B1} - r_{A1}r_{B2}) + 2r_{2\pi}(r_{A1}r_{B\pi} - r_{A\pi}r_{B1})], \quad \text{(A11)}$$

$$\xi_4 = -2m_A m_B r_{1\pi}r_{2\pi} + m_\pi^2(r_{12}r_{AB} - r_{A1}r_{B2} - r_{A2}r_{B1}) - 2r_{12}r_{A\pi}r_{B\pi} + r_{1\pi}(r_{A2}r_{B\pi} + r_{A\pi}r_{B2}) + r_{2\pi}(r_{A1}r_{B\pi} + r_{A\pi}r_{B1}), \quad \text{(A12)}$$

$$\xi_5 = \xi_4 - 2m_A m_B(m_\pi^2 r_{12} - 2r_{1\pi}r_{2\pi}), \quad \text{(A13)}$$

$$\xi_6 = 2[r_{1\pi}(r_{A2}r_{B\pi} - r_{A\pi}r_{B2}) + r_{2\pi}(r_{A1}r_{B\pi} - r_{A\pi}r_{B1})]. \quad \text{(A14)}$$

In the above expression, we have defined $r_{ij} \equiv p_i \cdot p_j$ with p_i and p_j, denoting any of the momenta of the external particles (that is $p_{i,j} = p_A, p_B, p_1, p_2, p_\pi$). Now, for the set of variables chosen in Sec. II, the scalar products r_{ij} involved in Eqs. (A9)–(A14) are given as follows:

$$r_{B1} = \frac{1}{2}(s_{B1} - m_B^2 - m_1^2),$$
$$r_{2\pi} = \frac{1}{2}(s_{2\pi} - m_2^2 - m_\pi^2), \quad \text{(A15)}$$

$$r_{B2} = \frac{1}{4}(\alpha_1 + \alpha_2 + \alpha_3 + \alpha_4),$$
$$r_{B\pi} = \frac{1}{4}(\alpha_1 - \alpha_2 + \alpha_3 - \alpha_4), \quad \text{(A16)}$$

$$r_{12} = \frac{1}{4}(\alpha_1 + \alpha_2 - \alpha_3 - \alpha_4),$$
$$r_{1\pi} = \frac{1}{4}(\alpha_1 - \alpha_2 - \alpha_3 + \alpha_4), \quad \text{(A17)}$$

$$r_{AB} = \frac{1}{2}(\alpha_5 + \alpha_6), \qquad r_{A1} = \frac{1}{2}(\alpha_5 - \alpha_6), \quad \text{(A18)}$$

$$r_{A2} = \frac{1}{2}(\alpha_7 + \alpha_8), \qquad r_{A\pi} = \frac{1}{2}(\alpha_7 - \alpha_8), \quad \text{(A19)}$$

$$\epsilon_{\mu\nu\lambda\rho}p_B^\mu p_1^\nu p_2^\lambda p_\pi^\rho = -\sqrt{s_{B1}s_{2\pi}}\beta_{B1}\beta_{2\pi}X\sin\theta_B\sin\theta_2\sin\phi, \quad \text{(A20)}$$

with the definitions

$$\alpha_1 = \frac{1}{2}(m_A^2 - s_{B1} - s_{2\pi}), \quad \text{(A21)}$$

$$\alpha_2 = X\beta_{2\pi}\cos\theta_2 + \left(\frac{m_2^2 - m_\pi^2}{s_{2\pi}}\right)\alpha_1, \quad \text{(A22)}$$

$$\alpha_3 = X\beta_{B1}\cos\theta_B + \left(\frac{m_B^2 - m_1^2}{s_{B1}}\right)\alpha_1, \quad \text{(A23)}$$

$$\alpha_4 = \left(\frac{m_B^2 - m_1^2}{s_{B1}}\right)\left(\frac{m_2^2 - m_\pi^2}{s_{2\pi}}\right)\alpha_1 + \left(\frac{m_B^2 - m_1^2}{s_{B1}}\right)X\beta_{2\pi}\cos\theta_2 + \left(\frac{m_2^2 - m_\pi^2}{s_{2\pi}}\right)X\beta_{B1}\cos\theta_B + \beta_{B1}\beta_{2\pi}(\alpha_1\cos\theta_B\cos_{\theta_2} - \sqrt{s_{B1}s_{2\pi}}\sin\theta_B\sin\theta_2\cos\phi), \quad \text{(A24)}$$

$$\alpha_5 = \frac{1}{2}(m_A^2 + s_{B1} - s_{2\pi}), \quad \text{(A25)}$$

$$\alpha_6 = (m_B^2 - m_1^2)\left(1 + \frac{\alpha_1}{s_{B1}}\right) + X\beta_{B1}\cos\theta_B, \quad \text{(A26)}$$

$$\alpha_7 = \frac{1}{2}(m_A^2 - s_{B1} + s_{2\pi}), \quad \text{(A27)}$$

$$\alpha_8 = (m_2^2 - m_\pi^2)\left(1 + \frac{\alpha_1}{s_{2\pi}}\right) + X\beta_{2\pi}\cos\theta_2, \quad \text{(A28)}$$

and

$$\lambda(a,b,c) = a^2 + b^2 + c^2 - 2(ab + bc + ac), \quad \text{(A29)}$$

$$X = \frac{\lambda(m_A^2, s_{B1}, s_{2\pi})^{1/2}}{2}, \qquad \beta_{B1} = \frac{\lambda(s_{B1}, m_B^2, m_1^2)^{1/2}}{s_{B1}},$$
$$\beta_{2\pi} = \frac{\lambda(s_{2\pi}, m_2^2, m_\pi^2)^{1/2}}{s_{2\pi}}. \quad \text{(A30)}$$

APPENDIX B: COMPARISON WITH DIRECT NARROW WIDTH APPROXIMATION COMPUTATION

For completeness and as a cross-check of our computation, we have verified that for the cases where we can distinguish the flavor of the charged lepton created as a

product of the decay of the resonant state or the channels with two identical external charged leptons, the results using the single-diagram-enhanced multichannel integration method can be reproduced by applying directly the narrow width approximation,

$$\mathrm{BR}(B_A \to B_B \ell_1^- \ell_2^- \pi^+) = \mathrm{BR}(B_A \to B_B \ell_1^- N) \times \Gamma(N \to \ell_2^- \pi^+)\tau_N/\hbar, \tag{B1}$$

where τ_N is the lifetime of the intermediate neutrino state. In this case, the partial decay width $\Gamma(N \to \ell_2^- \pi^+)$ can be computed straightforwardly by [12]

$$\Gamma(N \to \ell_2^- \pi^+) = \frac{G_F^2}{16\pi}|V_{ud}|^2|V_{\ell_2 N}|^2 f_\pi^2 m_N \lambda^{\frac{1}{2}}(m_N^2, m_{\ell_2}^2, m_\pi^2)[(1-x_{\ell_2})^2 - x_\pi(1+x_{\ell_2})], \tag{B2}$$

with $x_y \equiv m_y^2/m_N^2$, λ is the Källén function defined previously, and f_π is the pion decay constant. Regarding the subprocess $B_A(p_A) \to B_B(p_B)\ell_1^-(p_1)N(p_N)$ in Eq. (B1), the amplitude is given by

$$\mathcal{M}(B_A \to B_B \ell_1^- N) = -\frac{G_F}{\sqrt{2}} V_{us} V_{\ell_1 N} \langle B_B(p_B)|J_\mu|B_A(p_A)\rangle L^\mu, \tag{B3}$$

with J_μ hadronic previously defined in Eq. (2.6), and the leptonic current defined as follows:

$$L^\mu \equiv \bar{u}(p_1)\gamma^\mu(1-\gamma_5)v(p_N). \tag{B4}$$

The squared amplitude of Eq. (B3) is given by

$$\begin{aligned}|\mathcal{M}|^2 &= \mathcal{M}\mathcal{M}^\dagger \\ &= 32G_F^2|V_{us}|^2|V_{\ell_1 N}|^2[m_A m_B(g_1^2(q^2) - f_1^2(q^2)) + (f_1(q^2) - g_1(q^2))^2(p_1\cdot p_B)(p_A\cdot p_N) \\ &\quad + (f_1(q^2) + g_1(q^2))^2(p_1\cdot p_A)(p_B\cdot p_N)].\end{aligned} \tag{B5}$$

Now, by defining $s_{1N} \equiv (p_1+p_N)^2$ and $s_{1B} \equiv (p_1+p_B)^2$, the branching ratio can be expressed in terms of these two Lorentz invariants as follows:

$$\mathrm{BR}(B_A \to B_B \ell_1^- N) = \frac{G_F^2|V_{us}|^2|V_{\ell_1 N}|^2}{64\pi^3 m_A^3 \Gamma_{B_A}} \int_{s_{1B_{\min}}}^{s_{1B_{\max}}} \int_{s_{1N_{\min}}}^{s_{1N_{\max}}} \mathcal{F}(s_{1B}, s_{1N}) ds_{1N} ds_{1B}, \tag{B6}$$

where

$$\begin{aligned}\mathcal{F}(s_{1B}, s_{1N}) &= 2m_A m_B(s_{1N} - m_N^2 - m_1^2)\left[\frac{g_1^2(0)}{(1-\frac{s_{1N}}{m_{d_g}^2})^4} - \frac{f_1^2(0)}{(1-\frac{s_{1N}}{m_{d_f}^2})^4}\right] \\ &\quad + (s_{1B} - m_B^2 - m_1^2)(m_A^2 + m_N^2 - s_{1B})\left[\frac{f_1(0)}{(1-\frac{s_{1N}}{m_{d_f}^2})^2} - \frac{g_1(0)}{(1-\frac{s_{1N}}{m_{d_g}^2})^2}\right]^2 \\ &\quad + (m_1^2 + m_A^2 - s_{1B} - s_{1N})(s_{1B} + s_{1N} - m_N^2 - m_B^2)\left[\frac{f_1(0)}{(1-\frac{s_{1N}}{m_{d_f}^2})^2} + \frac{g_1(0)}{(1-\frac{s_{1N}}{m_{d_g}^2})^2}\right]^2,\end{aligned} \tag{B7}$$

and the phase space integration limits are

$$s_{1B}^{\pm} = m_A^2 + m_1^2 - s_{1N} - \frac{1}{2s_{1N}}\left[(m_A^2 - m_B^2 - s_{1N})(s_{1N} - m_1^2 + m_2^2) \pm \sqrt{\lambda(m_A^2, m_B^2, s_{1N})\lambda(s_{1N}, m_1^2, m_2^2)}\right], \tag{B8}$$

and

$$(m_1 + m_N)^2 \le s_{1N} \le (m_A - m_B)^2. \tag{B9}$$

Finally, the numerical values (central values) for the masses, lifetimes, and Cabibbo-Kobayashi-Maskawa matrix elements used in our numerical analysis are reported in [51].

[1] N. Cabibbo, Phys. Rev. Lett. **10**, 531 (1963).
[2] Y. Hara, Y. Nambu, and J. Schechter, Phys. Rev. Lett. **16**, 380 (1966).
[3] G. Bunce, R. Handler, R. March, P. Martin, L. Pondrom, M. Sheaff, K. J. Heller, O. Overseth, P. Skubic, T. Devlin *et al.*, Phys. Rev. Lett. **36**, 1113 (1976).
[4] A. Le Yaouanc, O. Pene, J. C. Raynal, and L. Oliver, Nucl. Phys. **B149**, 321 (1979).
[5] L. S. Littenberg and R. E. Shrock, Phys. Rev. D **46**, R892 (1992).
[6] D. Rajaram *et al.* (HyperCP Collabortion), Phys. Rev. Lett. **94**, 181801 (2005).
[7] M. Raggi (NA48/2 Collaboration), Nuovo Cimento C **38**, 132 (2016).
[8] R. Aaij *et al.* (LHCb Collaboration), Phys. Rev. Lett. **120**, 221803 (2018).
[9] A. A. Affolder *et al.* (KTeV E832/E799 Collaborations), Phys. Rev. Lett. **82**, 3751 (1999).
[10] H. B. Li, Front. Phys. **12**, 121301 (2017); **14**, 64001(E) (2019).
[11] M. Ablikim *et al.* (BESIII Collaboration), Phys. Rev. D **103**, 052011 (2021).
[12] A. Atre, T. Han, S. Pascoli, and B. Zhang, J. High Energy Phys. 05 (2009) 030.
[13] G. L. Castro and N. Quintero, Phys. Rev. D **87**, 077901 (2013).
[14] G. Lopez Castro and N. Quintero, Phys. Rev. D **85**, 076006 (2012); **86**, 079904(E) (2012).
[15] D. Milanes, N. Quintero, and C. E. Vera, Phys. Rev. D **93**, 094026 (2016).
[16] G. Cvetic and C. S. Kim, Phys. Rev. D **94**, 053001 (2016); **95**, 039901(E) (2017).
[17] G. Cvetic and C. S. Kim, Phys. Rev. D **96**, 035025 (2017); **102**, 019903(E) (2020); **102**, 039902(E) (2020).
[18] A. Abada, V. De Romeri, M. Lucente, A. M. Teixeira, and T. Toma, J. High Energy Phys. 02 (2018) 169.
[19] Y. Cai, T. Han, T. Li, and R. Ruiz, Front. Phys. **6**, 40 (2018).
[20] J. Mejia-Guisao, D. Milanés, N. Quintero, and J. D. Ruiz-Alvarez, Phys. Rev. D **97**, 075018 (2018).
[21] J. Mejia-Guisao, D. Milanes, N. Quintero, and J. D. Ruiz-Alvarez, Phys. Rev. D **96**, 015039 (2017).
[22] H. Yuan, T. Wang, Y. Jiang, Q. Li, and G. L. Wang, J. Phys. G **45**, 065002 (2018).
[23] H. l. Li, P. c. Lu, C. f. Qiao, Z. g. Si, and Y. Wang, Chin. Phys. C **43**, 023101 (2019).
[24] D. Milanés and N. Quintero, Phys. Rev. D **98**, 096004 (2018).
[25] G. Cvetič and C. S. Kim, Phys. Rev. D **100**, 015014 (2019).
[26] D. Das and J. Das, Phys. Rev. D **105**, 013009 (2022).
[27] D. Das and J. Das, Phys. Rev. D **103**, 073001 (2021).
[28] G. Zhang and B. Q. Ma, Phys. Rev. D **103**, 033004 (2021).
[29] E. J. Chun, A. Das, S. Mandal, M. Mitra, and N. Sinha, Phys. Rev. D **100**, 095022 (2019).
[30] A. A. Alves, Junior, M. O. Bettler, A. Brea Rodríguez, A. Casais Vidal, V. Chobanova, X. Cid Vidal, A. Contu, G. D'Ambrosio, J. Dalseno, F. Dettori *et al.*, J. High Energy Phys. 05 (2019) 048.
[31] C. Barbero, G. Lopez Castro, and A. Mariano, Phys. Lett. B **566**, 98 (2003).
[32] C. Barbero, L. F. Li, G. Lopez Castro, and A. Mariano, Phys. Rev. D **76**, 116008 (2007).
[33] C. Barbero, L. F. Li, G. López Castro, and A. Mariano, Phys. Rev. D **87**, 036010 (2013).
[34] G. Hernández-Tomé, G. L. Castro, and D. Portillo-Sánchez, Phys. Rev. D **105**, 113001 (2022).
[35] A. Abada, C. Hati, X. Marcano, and A. M. Teixeira, J. High Energy Phys. 09 (2019) 017.
[36] J. Zhang, T. Wang, G. Li, Y. Jiang, and G. L. Wang, Phys. Rev. D **103**, 035015 (2021).
[37] R. M. Godbole, S. P. Maharathy, S. Mandal, M. Mitra, and N. Sinha, Phys. Rev. D **104**, 9 (2021).
[38] E. Fernández-Martínez, X. Marcano, and D. Naredo-Tuero, J. High Energy Phys. 03 (2023) 057.
[39] A. García and P. Kielanowski, *The Beta Decay of Hyperons*, Lectures Notes in Physics Vol. 222 (Springer–Verlag, Berlin, 1985).
[40] P. G. Ratcliffe, Czech. J. Phys. **54**, B11 (2004), arXiv:hep-ph/0402063.
[41] F. Schlumpf, Phys. Rev. D **51**, 2262 (1995).
[42] V. Mateu and A. Pich, J. High Energy Phys. 10 (2005) 041.
[43] A. Sirlin, Nucl. Phys. **B161**, 301 (1979).
[44] P. G. Ratcliffe, Phys. Lett. B **365**, 383 (1996).
[45] F. Maltoni and T. Stelzer, J. High Energy Phys. 02 (2003) 027.
[46] N. Cabibbo and A. Maksymowicz, Phys. Rev. **137**, B438 (1965); **168**, 1926(E) (1968).
[47] E. Fernandez-Martinez, J. Hernandez-Garcia, and J. Lopez-Pavon, J. High Energy Phys. 08 (2016) 033.
[48] E. Cortina Gil *et al.* (NA62 Collaboration), Phys. Lett. B **797**, 134794 (2019).
[49] E. Cortina Gil *et al.* (NA62 Collaboration), Phys. Lett. B **830**, 137172 (2022).
[50] A. Denner, H. Eck, O. Hahn, and J. Kublbeck, Nucl. Phys. **B387**, 467 (1992).
[51] P. A. Zyla *et al.* (Particle Data Group), Prog. Theor. Exp. Phys. **2020**, 083C01 (2020).